Regulation of the Transport and Protein Levels of the Inositol Phosphorylceramide Mannosyltransferases Csg1 and Csh1 by the Ca^{2+}-binding Protein Csg2*

Satoshi Uemura[‡§¶], Akio Kihara[¶1], Soichiro Iwaki[¶], Jin-ichi Inokuchi[‡§¶], and Yasuyuki Igarashi[¶‖]

From the [‡]Division of Glycopathology, Institute of Molecular Biomembrane and Glycobiology, Tohoku Pharmaceutical University, 4-4-1, Komatsushima, Aoba-ku, Sendai, Miyagi 981-8558, Japan, the [§]Core Research for Evolutional Science and Technology Program (CREST), Japan Science and Technology Agency (JST), the [¶]Laboratory of Biomembrane and Biofunctional Chemistry, Faculty of Pharmaceutical Sciences, Hokkaido University, Kita 12-jo, Nishi 6-choume, Kita-ku, Sapporo 060-0812, Japan, and the [‖]Laboratory of Biomembrane and Biofunctional Chemistry, Faculty of Advanced Life Science, Hokkaido University, Kita 21-jo, Nishi 11-choume, Kita-ku, Sapporo 001-0021, Japan

Running Title: Regulation of Csg1 and Csh1 by Csg2

Address correspondence to: Akio Kihara, Laboratory of Biomembrane and Biofunctional Chemistry, Faculty of Pharmaceutical Sciences, Hokkaido University, Kita 12-jo, Nishi 6-choume, Kita-ku, Sapporo 060-0812, Japan, Tel: +81-11-706-3971; Fax: +81-11-706-4986; E-mail: kihara@pharm.hokudai.ac.jp

Complex sphingolipids in yeast are known to function in cellular adaptation to environmental changes. One of the yeast complex sphingolipids, mannosylinositol phosphorylceramide (MIPC), is produced by the redundant inositol phosphorylceramide (IPC) mannosyltransferases Csg1 and Csh1. The Ca^{2+}-binding protein Csg2 can form a complex with either Csg1 or Csh1 and is considered to act as a regulatory subunit. However, the role of Csg2 in MIPC synthesis has remained unclear. In this study, we found that Csg1 and Csh1 are *N*-glycosylated with 'core-type' and 'mannan-type' structures, respectively. Further identification of the glycosylated residues suggests that both Csg1 and Csh1 exhibit membrane topology with their C-termini in the cytosol and their mannosyltransferase domains in the lumen. After complexing with Csg2, both Csg1 and Csh1 function in the Golgi, then are delivered to the vacuole for degradation. However, uncomplexed Csh1 cannot exit from the endoplasmic reticulum. We also demonstrated that Ca^{2+} stimulates IPC-to-MIPC conversion, due to a Csg2-dependent increase in Csg1 levels. Thus, Csg2 has several regulatory functions for Csg1 and Csh1, including stability, transport, and gene expression.

Glycosphingolipids (GSLs)[2] are ubiquitous and abundant components of the eukaryotic plasma membrane that function in numerous cellular processes, such as proliferation, differentiation, and adhesion (1). They are also involved in the formation of membrane lipid microdomains (lipid rafts), which serve as platforms for effective signal transduction (2). In mammals, several hundred GSLs differing in number and/or type of sugar chains constitute some of the complex sphingolipids. In contrast, the sphingolipid composition in the yeast *Saccharomyces cerevisiae* is quite simple, existing of only three *myo*-inositol-containing complex sphingolipids.

The simplest of the yeast sphingolipids, inositol phosphorylceramide (IPC), which is essential for cell growth (3, 4), comprises a common ceramide backbone carrying a

phosphoinositol. There are five IPCs (IPC-A, -B, -B', -C, and -D), which differ in the position and/or number of hydroxyl groups within the ceramide moiety (5-7). The other two yeast sphingolipids are mannose-containing GSLs that are not required for normal cell growth, though their loss results in altered sensitivities to several drugs (8-11). Mannosylinositol phosphorylceramide (MIPC) is formed by the addition of mannose to IPC, and addition of another phosphoinositol generates mannosyldiinositol phosphorylceramide ($M(IP)_2C$).

MIPC synthesis is catalyzed by either of two homologous IPC mannosyltransferases, Csg1 and Csh1, which prefer different IPC species as substrates (12, 13). Cells carrying a double mutation, Δ*csg1* Δ*csh1*, are sensitive to external Ca^{2+} (5, 12, 14), suggesting a role for the GSLs in cellular stress response. We recently demonstrated that the Ca^{2+}-binding protein Csg2 (14, 15), interacts with both Csg1 and Csh1 (12). Our Δ*csg1* Δ*csg2* cells had no MIPC synthase activity, and introduction of a Δ*csg2* mutation into the Δ*csh1* cells also resulted in a significant reduction in activity (12). Thus, interaction with Csg2 is essential for the activity of Csh1 and is quite important for that of Csg1.

The existence of the Ca^{2+}-binding regulatory subunit Csg2 and two different catalytic subunits, Csg1 and Csh1, implies that IPC-to-MIPC conversion is a highly regulated process. However, the exact functions of Csg2 and Ca^{2+} in MIPC synthesis remain unclear. In the present study, we report that Csg2 functions in the production, stability, and transport of Csg1 and/or Csh1. In addition, we found that Ca^{2+} treatment increases Csg1 levels in a Csg2-dependent manner and enhances MIPC synthesis.

Experimental Procedures

Yeast Strains and Media — *Saccharomyces cerevisiae* strains used are listed in Table I. The Δ*csg2*::*URA3* cells were constructed by replacing the 0.41 kb EcoRI-HincII region in the *CSG2* gene with *URA3* marker. The Δ*pep4*::*LEU2* cells were constructed as described elsewhere (16). The Δ*prb1*::*KanMX4* cells were constructed by replacing the entire open reading frame with the *KanMX4* marker. Cells were grown either in YPD medium (1% yeast extract, 2% peptone, and 2% glucose) or in synthetic complete (SC) medium (0.67% yeast nitrogen base (Sigma, St. Louis, MO) and 2% glucose) containing nutritional supplements.

The chromosomal *CSG1* gene was tagged at its 3'-terminus with three copies of a FLAG (3xFLAG) epitope by replacing the *CSG1* gene with a fragment containing both the *CSG1-3xFLAG* and a *HIS3* marker. To produce the DNA fragment used for this homologous recombination, an ~ 1 kb region of chromosomal DNA covering the 3'-half and 3'-downstreasm region of the *CSG1* gene was amplified by PCR using the primers 5'-GGAAGCAGTACAAAAGATGGCGC-3' and 5'-CCCACACACGGTTGTTATCCTAG-3'. The amplified DNA was cloned into pGEM-T Easy (Promega, Madison, WT), generating the pSU74 plasmid. Then, the termination codon of the *CSG1* gene in the plasmid was replaced with an XbaI site by site-directed mutagenesis using a QuikChange™ kit (Stratagene, La Jolla, CA) and the primers 5'-GGGAAATAACAGCTCGTCTAGAAATG GTATGACTCCAAC-3' and 5'-GTTGGAGTCATACCATTTCTAGACGAG CTGTTATTTCCC-3', creating pSU78. Finally, the 1.8 kb SpeI fragment of pAK453 containing the *3xFLAG* tag and the *HIS3* marker was inserted into the XbaI site of pSU78. The generated *CSG1-3xFLAG-HIS3* construct was

amplified by PCR and used for homologous recombination. The *CSH1* and *CSG2* genes were similarly tagged with *3xFLAG*.

Plasmids — The pSU8 (*CSG2-3xHA*, *LEU2* marker, 2 μ), pSU30 (*CSG1-HIS$_6$-MYC*, *HIS3* marker, 2 μ), and pSU41 (*CSH1-HIS$_6$-MYC*, *HIS3*, 2 μ) plasmids, encoding Csg2 C-terminally tagged with triple HA (3xHA) (Csg2-3xHA), Csg1 C-terminally tagged with His_6 and Myc (Csg1-His_6-Myc), and Csh1-His_6-Myc, respectively, have been described previously (12). Glycosylation mutants of *CSG1* (*CSG1-N224Q-HIS$_6$-MYC*, pSU145) and *CSH1* (*CSH1-N51Q-HIS$_6$-MYC*, pSU108; *CSH1-N247Q-HIS$_6$-MYC*, pSU109; *CSH1-N51/247Q-HIS$_6$-MYC*, pSU193) were created from a pSU30 or pSU41 plasmid by site-directed mutagenesis using the QuikChange™ kit. Two complementary oligonucleotides were used to construct each mutant. The sequences of the sense oligonucleotides (with mutated nucleotides underlined) were 5'-TGGCGCATACCTAAGCAGGGGACAGT AAGAATC-3' (*CSG1-N224Q-HIS$_6$-MYC*), 5'-CCCAATGGCTTCCAGTCAACATTCTATGA G-3' (*CSH1-N51Q-HIS$_6$-MYC*), and 5'-GATTATAAAATGCATCAGAATTCTTTTTT CTC-3' (*CSH1-N247Q-HIS$_6$-MYC*).

Immunoprecipitation — Yeast strains were grown in YPD medium at 30˚C to 1.0 A_{600} unit. Cells were suspended in buffer A (50 mM Tris-HCl (pH 7.5), 150 mM NaCl, 10% glycerol, 4 M urea, 1 mM phenylmethylsulfonyl fluoride (PMSF), and 1X Complete™ protease inhibitor mixture (EDTA free; Roche Diagnostics, Indianapolis, IN)) and vigorously mixed with glass beads for 10 min at 4˚C. After removal of cell debris and glass beads by centrifugation at 500 x g for 5 min at 4˚C, the supernatant (total cell lysates) was centrifuged at 100,000 x g for 1 h at 4˚C. The precipitates (integral membrane proteins) were suspended in buffer B (50 mM Tris-HCl (pH 7.4), 150 mM NaCl, 2 mM NaF, 1 mM EDTA, 1 mM ethylene glycol bis (2-aminoethyl ether)-tetra acetic acid, 1% Triton X-100, 1 mM PMSF, and 1X Complete™) and incubated overnight at 4˚C with an anti-FLAG M2 or anti-Myc (A7470) agarose conjugate (Sigma). The agarose beads were then washed three times with washing buffer (20 mM Tris-HCl (pH 7.5), 137 mM NaCl, and 0.05% Tween 20), and bound proteins were eluted with 2X sample buffer (125 mM Tris-HCl (pH 6.8), 4% SDS, 20% glycerol, and a trace amount of bromophenol blue). The immunoprecipitates were treated with 2-mercaptoethanol (final concentration, 5%) and boiled for 5 min.

Sucrose gradient fractionation — Sucrose gradient fractionation was performed as described elsewhere (17), with minor modifications. Briefly, approximately 4 x 10^9 cells were harvested, suspended in 10 ml buffer C (100 mM Tris-HCl (pH 9.4) and 40 mM 2-mercaptoethanol), and incubated at room temperature for 10 min. After centrifugation, cells were resuspended in 10 ml buffer D (50 mM Tris-HCl (pH 7.5) and 1.2 M sorbitol), and incubated at 30ºC for 30 min with 1 mg Zymolyase 100T (Seikagaku Corp., Tokyo, Japan). The resulting spheroplasts were washed with 10 ml buffer D and lysed in lysis buffer (20 mM HEPES-NaOH (pH 7.5), 0.8 M sorbitol, 2 mM $MgCl_2$, 1X Complete^{TM}, 1 mM PMSF, and 1 mM dithiothreitol) by passaging through a 27-gauge needle four times. Unlysed cells were removed by centrifugation at 1,000 x *g* for 5 min, and the supernatant was recovered and saved. This lysis step was repeated two more times. All of the supernatants were pooled and then centrifuged (10,000 x *g*, 10 min), yielding a final

supernatant. The cell supernatant (0.4 ml) was loaded onto a step sucrose gradient (22, 26, 30, 34, 38, 42, 46, 50, 54, 60%, and 75% (wt/vol) sucrose, each in 0.35 ml buffer (10 mM HEPES-NaOH (pH 7.5), 2 mM $MgCl_2$, 1X Complete™, 1 mM PMSF, and 1 mM dithiothreitol). After Samples were centrifuged at 250,000 x *g* for 2.5 h at 4˚C, 8 fractions (0.53 ml each) were collected from top to bottom. Each fraction was diluted with two volumes of lysis buffer, and membrane proteins were collected by centrifugation at 100,000 x *g* for 30 min at 4˚C. The proteins were suspended in 2X sample buffer, and subjected to immunoblotting.

Deglycosylation by Peptide N-glycosidase (PNGase) F — Removal of *N*-glycans was performed on integral membrane proteins or on the immunoprecipitates using PNGase F (New England Biolab, Beverly, MA) for 1 h at 37˚C, according to the manufacturer's instruction.

Immunoblotting — Immunoblotting was performed as described previously (18). The anti-FLAG antibody M2 (1.4 μg/ml; Stratagene), anti-Myc antibody PL14 (2 μg/ml; Medical & Biological Laboratories, Nagoya, Japan), anti-Dpm1 antibody 5C5 (2 μg/ml; Invitrogen, Carlsbad, CA), and an anti-Anp1 antiserum (1:4000 dilution; a gift from Dr. Sean Munro, Medical Research Council Laboratory of Molecular Biology, Cambridge, UK) (19) were used as primary antibodies. HRP-conjugated anti-mouse or anti-rabbit IgG $F(ab')_2$ fragment (both from GE Healthcare Bio-Sciences, Piscataway, NJ, and diluted 1:5000) was used as the secondary antibody. Labeling was detected using ECL™ (GE Healthcare Bio-Sciences), ECL™ plus kit (GE Healthcare Bio-Sciences), or Lumi-Light^{PLUS} Western Blotting Substrate (Roche Diagnostics).

Real-time quantitative PCR — Total RNA was isolated using the YeaStar RNA Kit™ (Zymo Research, Orange, CA) according to the manufacturer's manual. cDNA was prepared from 5 μg total RNA using a first-strand cDNA synthesis kit for reverse transcription-polymerase chain reaction (AMV) (Roche Diagnostics) according to the manufacture's protocol. Real-time PCR was performed using a TaqMan PCR kit on an Applied Biosystems 7500 Real Time PCR system (Applied Biosystems, Foster City, CA). TaqMan universal PCR master mix, primers (*CSG1*, 5'-GAACGGGACAGTAAGAATCCTACAA-3' and 5'-CATGAAGAGCCTTTAGTAATGGAGAA-3'; *CSH1*, 5'-GAGGGCGGATGCAATACG-3' and 5'-CAACCATCATCCAAGTCAATGTAAA-3'; *CSG2*, 5'-AACGGCGACAACGGAAACT-3' and 5'-GCAGCCACGAAGCAAAATACA-3'; *ACT1*, 5'-TGGATTCCGGTGATGGTGTT-3' and 5'-AAATGGCGTGAGGTAGAGAGAAA-3'), and probes (*CSG1*, 5'-CTGCTTACTACAAGATGCATAGTTATTCAT-3'; *CSH1*, 5'-TTTCATCCTTTCGCATTATGGT-3'; *CSG2*, 5'-AAGTTCATTAACCTTCTATCTGACCTTT-3'; *ACT1*, 5'-CTCACGTCGTTCCAATTTACGCT-3') were purchased from Applied Biosystems. The 50 μl PCR mixtures included 5 μl reverse transcription product, 2X TaqMan Universal PCR Master Mix, 0.25 μM TaqMan probe, 0.9 μM forward primer, and 0.9 μM reverse primer. The reactions were incubated in a 96-well plate at 95˚C for 10 min, followed by 40 cycles at 95˚C for 15 s, and 60˚C for 1 min. All reactions were run in triplicate.

In Vivo [^{3}H]Dihydrosphingosine (DHS) Labeling — [^{3}H]DHS labeling assay was performed as described previously (12).

RESULTS

N-glycosylation in Csg1 and Csh1 — To detect endogenous Csg1 and Csh1, we inserted a 3xFLAG tag into the 3'-termini of the endogenous *CSG1* and *CSH1* genes, generating SUY69 and SUY73 cells, respectively. The tagged proteins were immunoprecipitated and detected by immunoblotting with anti-FLAG antibodies. Csg1-3xFLAG (predicted molecular mass 47 kDa) was detected as two bands, a major 46 kDa band and a weak 48 kDa band (Fig. 1*A*). Consistent with a previous report (13), the upper 48 kDa band was determined to be an *N*-glycosylated form, since it shifted to 46 kDa upon treatment with PNGase F. Similarly, Csh1-3xFLAG (predicted molecular mass 47 kDa) was detected as several bands of 47.5 kDa, 49 kDa, and a broad band of 55-70 kDa (Fig. 1*B*). All the bands converged at 46 kDa upon treatment with PNGase F (Fig. 1*B*). These results indicate that both Csg1 and Csh1 carry *N*-glycans.

Effects of Csg2 on the glycosylation status of Csh1 — Recently, we reported that Csg2 forms a complex with Csg1 or Csh1 (12). Therefore, we next examined the effects of Csg2 on the glycosylation status of Csg1 and Csh1. Neither the gel mobility nor protein levels of Csg1-3xFLAG differed in the Δ*csg2* cells compared to those in cells bearing the wild-type *CSG2* (Fig. 2*A*). In contrast, the broad bands of 55-70 kDa representing Csh1-3xFLAG were completely converted in the Δ*csg2* mutant to the 49 kDa band (Fig. 2*A*), which may have the endoplasmic reticulum (ER) "high mannose-type" glycan as discussed below.

We also investigated the glycosylation status of overproduced Csg1 and Csh1. Both proteins were expressed as C-terminally His_6-Myc-tagged proteins under their own promoters from multicopy (2 μ) plasmids. As shown in Fig. 2*B*, their glycosylation status was similar to the endogenously expressed proteins. Csg1-His_6-Myc was detected as 46 kDa and 48 kDa bands. PNGase F treatment demonstrated that the 48 kDa band but not the 46 kDa band again represented a glycosylated form (data not shown). Csh1-His_6-Myc was observed as 49 kDa and broad, 55-70 kDa bands (Fig. 2*B*), all of which shifted to 46 kDa with PNGase F treatment (data not shown). Next, we investigated the effects of co-overproduction of Csg2-3xHA on the glycosylation status and protein levels of Csg1-His_6-Myc and Csh1-His_6-Myc. Although overproduction of Csg2-3xHA had little effect on the ratio of glycosylated to nonglycosylated forms of Csg1-His_6-Myc, it did cause increases in the protein levels of both forms (Fig. 2*B*). In contrast, Csg2-3xHA overproduction significantly affected the glycosylation status of Csh1-His_6-Myc. The 49 kDa band of Csh1-His_6-Myc was diminished, and, concomitantly, the broad 55-70 kDa was enhanced. These results suggest that interaction with Csg2 affects the protein level and glycosylation of Csg1 and Csh1, respectively.

Modification of Csh1 with the mannan-type glycosylation — Two different *N*-glycan structures have been found in yeast proteins (20, 21). One is the 'mannan-type' structure, which consists of a backbone of about 50 mannose residues with short side branches. Several cell wall and periplasm proteins carry this type of modification. On the other hand, proteins localized in the ER, Golgi, endosomes, vacuole, or plasma membrane often have a much

smaller 'core-type' structure with only a few mannoses (Fig. 3*A*). The much higher molecular mass of Csh1-3xFLAG (55-70 kDa; Fig. 1*B*) compared to the predicted mass (47 kDa) is characteristic of mannan-type modification with dozens of sugars. To confirm this, we expressed Csh1-His_6-Myc and Csg1-His_6-Myc in mutants lacking Van1, an enzyme involved in the synthesis of mannan-type structures (Fig. 3*A*). As shown in Fig. 3*B*, the gel mobility of Csg1-His_6-Myc was unchanged in the Δ*van1* cells. In contrast, the broad 55-70 kDa bands of Csh1-His_6-Myc observed in the wild-type cells were diminished in the Δ*van1* mutants, but a 51 kDa band appeared, which may carry an incomplete mannan-type structure (Fig. 3*C*). These results suggest that Csh1 is *N*-glycosylated with a 'mannan-type' structure, whereas Csg1 may be modified with 'core-type' glycosylation.

Defective trafficking of Csh1 from the ER to the Golgi by CSG2 deletion — In Δ*csg2* cells, Csh1-3xFLAG, normally a broad 55-70 kDa band, appeared as a 49 kDa band (Fig. 2*A*). It is highly likely that the 49 kDa band carries *N*-glycans of the high mannose-type, which are found in the ER and are the precursors of the mannan-type structure. Mannan-type modification is known to occur in the Golgi apparatus (21), so the loss of the mannan-type modification on Csh1 in the Δ*csg2* cells suggests that Csh1 cannot exit the ER without interacting with Csg2. To test this further, we examined the subcellular distribution of Csh1 in wild-type (*CSG2*$^+$) and Δ*csg2* cells by sucrose gradient fractionation. As shown Fig. 4, Csh1-3xFLAG carrying N-glycans of the mannan-type (Csh1-3xFLAG (M)) and high mannose-type (Csh1-3xFLAG (H)) were co-fractionated with the Golgi marker Anp1 and the ER marker Dpm1, respectively, in wild-type cells (*CSG2*$^+$). In contrast, most of Csh1-3xFLAG in the Δ*csg2* mutant cells carried N-glycans of the high mannose-type (Csh1-3xFLAG (H)) and co-fractionated with Dpm1 (Fig. 4). These results indicate that Csh1 cannot exit the ER without Csg2.

The effects of Csg2 on the degradation and transport of Csg1 and Csh1 – Integral membrane proteins like Csg1 and Csh1 can be degraded either by the proteasome, after dislocation from the ER membrane (ER-associated degradation (ERAD)) (22), or by vacuolar proteases, after transport to the vacuoles. To further examine the effect of Csg2 on the stability and transport of Csg1 and Csh1, we constructed a double null mutant for *PEP4* and *PRB1*, which each encodes a major vacuolar protease. In the Δ*pep4* Δ*prb1* mutant, the amount of endogenously expressed Csg1-3xFLAG was increased (Fig. 5*A*), suggesting that Csg1 is delivered to the vacuole for degradation. In addition, the pattern and intensity of this band were similar in the Δ*csg2* Δ*pep4* Δ*prb1* mutant, indicating that free Csg1 follows the same fate as that of Csg1 complexed with Csg2. The Csh1 level was also increased in the Δ*pep4* Δ*prb1* mutant (Fig. 5*B*), but strikingly so, implying that it is normally degraded in the vacuole. However, introduction of the Δ*csg2* mutation into the Δ*pep4* Δ*prb1* cells greatly reduced the Csh1-3xFLAG to levels similar to those observed in wild-type (*PEP4*$^+$ *PRB1*$^+$ *CSG2*$^+$) cells. This supports the contention that free Csh1 cannot exit the ER, since mutations in the vacuolar protease had no effect on Csh1 levels in the absence of Csg2. Free Csh1 may instead be subjected to rapid degradation by ERAD. In summary, Csg2 exerts different effects on the transport of Csg1 and Csh1.

Determination of N-glycosylation sites in

Csh1 and Csg1 — Csh1 and Csg1 exhibit similar hydrophobic profiles and are predicted by the TopPredII 1.1 program (23) to be integral membrane proteins with up to three transmembrane segments (Fig. 6*A;* H1 to H3). In addition, Csh1 and Csg1 contain two (Asn-51 and Asn-247) and six (Asn-224, Asn-295, Asn-298, Asn-370, Asn-379, and Asn-380) potential *N*-glycosylation sites, respectively (Fig. 6*A*). To determine which of the Csh1 sites are *N*-glycosylation sites, Asn to Gln mutants (N51Q, N247Q, and N51Q/247Q) were constructed and overexpressed in yeast cells as His_6-Myc-tagged proteins. Both N51Q and N247Q mutants exhibited faster migration than that of the wild-type protein, and the N51Q/N247Q double substitution resulted in a single 46 kDa band, corresponding to the nonglycosylated form (Fig. 6*B*). These results indicate that both Asn-51 and Asn-247 in Csh1 are modified by glycosylation. *N*-glycosylation occurs only in the ER lumen. Therefore, our results indicate that both Asn-51 and Asn-247 are localized in the lumenal side and, thus, the H2 region must not traverse the membrane. The proposed topology model is illustrated in Fig. 6*C*.

Since Csg1 shares high similarities with Csh1 in amino acid sequence and hydrophobic profile, it is reasonable to consider that Csg1 exhibits similar transmembrane topology. Of the six potential *N*-glycosylation sites, only Asn-224 is predicted to be in the lumenal domain. Thus, we created an N224Q mutant and examined its glycosylation status. The N224Q mutant Csg1 was detected as a single 46 kDa band, in contrast to wild-type Csg1-His_6-myc, which was detected as two bands (Fig. 6*B*). This result indicates that Asn-224 in Csg1 is indeed modified by glycosylation. Thus, it is highly likely that Csg1 exhibits the same transmembrane topology as Csh1 (Fig. 6*C*).

Enhanced synthesis of MIPC in the presence of Ca^{2+} — Since Csg2 has a Ca^{2+}-binding domain, we next examined whether Ca^{2+} treatment caused changes in the protein levels of Csg1, Csh1 and Csg2. Cells were treated with 0, 0.1, 1, 10, or 100 mM $CaCl_2$, and endogenously expressed Csg1-3xFLAG, Csh1-3xFLAG, and Csg2-3xFLAG were examined by immunoblotting following PNGase F treatment to remove *N*-glycans. Treatment with Ca^{2+} did result in dose-dependent increases in Csg1-3xFLAG (Fig. 7*A*). However, treatment was less effective in the Δ*csg2* cells, suggesting that Csg2 is involved in this process. In contrast, endogenously expressed Csh1-3xFLAG and Csg2-3xFLAG were nearly unchanged by treatment with Ca^{2+} (Fig. 7*A*).

To investigate whether the increases in protein levels were due to enhanced gene expression, we performed real-time PCR analyses. The mRNA levels of *CSG1* were increased upon treatment with Ca^{2+}, in a dose-dependent manner (Fig. 7*B*). Again, however, Ca^{2+} treatment had no significant effect on *CSH1* and *CSG2* mRNA levels. Thus, the increases in Csg1 protein levels could be explained by enhanced gene expression.

Next, we investigated whether the up-regulation of these proteins by Ca^{2+} affects MIPC synthesis. Cells were treated with increasing concentrations of Ca^{2+} then labeled with [^{3}H]DHS. As reported previously (12, 24, 25), [^{3}H]DHS was metabolized to IPC, MIPC, and $M(IP)_2C$ with various ceramide species (A-, B-, B'-, C, and D-type). Treatment of wild-type cells with Ca^{2+} caused a dose-dependent reduction in IPC-C levels and increases in MIPC-A and MIPC-C levels (Fig. 8), suggesting that IPC-to-MIPC conversion was stimulated by the Ca^{2+}. $M(IP)_2C$-C was also increased, probably due to the increase in the substrate

MIPC-C. Increases in IPC-A and IPC-D levels were also observed, although the mechanism behind this was unclear. These results suggest that exogenous Ca^{2+} causes a change in sphingolipid composition by affecting the activities of several sphingolipid-metabolizing enzymes, including MIPC synthases.

DISCUSSION

Yeast sphingolipids contain only one mannose, the addition of which is catalyzed by one of two distinct IPC mannosyltransferase complexes, Csg1-Csg2 or Csh1-Csg2. The product itself, MIPC, and its metabolite $M(IP)_2C$ appear to function in cellular adaptation to environmental changes like high Ca^{2+} levels, oxidative stress, and drug treatment (5, 8-12, 14, 26). Therefore, IPC-to-MIPC conversion may be a key regulatory step for determining cellular sphingolipid composition. Indeed, we found that this step is stimulated in the presence of Ca^{2+} (Fig. 8). As a result, IPC levels were reduced, and MIPC/$M(IP)_2C$ levels were increased. The enhanced IPC-to-MIPC conversion in the presence of Ca^{2+} was nicely explained by increases in the mRNA and protein levels of *CSG1* but not of *CSH1* (Fig. 7 *A* and *B*).

Csg2 was found to be involved in the Ca^{2+}-dependent Csg1 increase (Fig. 7*A*). In addition, overproduction of Csg2 also resulted in an increase in Csg1 level (Fig. 2*B*). Thus, a signaling pathway that transduces signal from Csg2 to the *CSG1* gene expression may exist. Binding of Ca^{2+} to Csg2 or Csg2 overproduction might enhance the signal, leading to increases in *CSG1* mRNA.

Secreted proteins and those localized in the ER, Golgi, endosomes, plasma membrane, and vacuole are synthesized by the ER-bound ribosome. Only properly folded proteins can exit from the ER, while proteins that are misfolded due to mutation or misassembly into a proper complex are removed by an ER quality control system, the so-called ERAD (27-29). In the present study, we determined that Csh1 is unable to exit from the ER unless it forms a complex with Csg2 (Figs. 2, 4, and 5*B*); apparently free Csh1 is removed by ERAD. In contrast, free Csg1 was transported to the vacuole via the Golgi, in a similar fashion to Csg1 complexed with Csg2 (Figs. 2*A* and 5*A*). This suggests that Csg1 can fold into its proper conformation to some extent in the absence of Csg2. Consistent with these results, Csh1 had no activity in the Δ*csg2* cells, whereas Csg1 retained activity, albeit weak activity (12).

Herein, we also identified the *N*-glycosylated amino acid residues of Csg1 and Csh1. Based on these results, we proposed membrane topology for both Csg1 and Csh1, as illustrated in Fig. 6*C*. Csg1 and Csh1 are integral membrane proteins with two transmembrane domains (H1 and H3) or perhaps one, if H1 acts as a signal sequence. At present, it is not clear whether H1 is removed from the mature Csg1 or Csh1 as a signal sequence or acts as a transmembrane domain. In our model the C-termini are localized in the cytosol, whereas the conserved mannosyltransferase domains are in the lumen. However, this topology differs from a previously proposed Csg1 topology, in which both H2 and H3 span the membrane with N_{lumen}/C_{cyto} (N-terminus, lumen; C-terminus, cytosol) and N_{cyto}/C_{lumen} orientation, respectively (13). This model was based on two principles. First, the authors claimed that Csg1 contains five potential glycosylation sites, all of which are preceded by the H2 region. Thus, they concluded that the C-terminal hydrophilic tail must be glycosylated, although they did not test this experimentally. However, we found an additional potential glycosylation site (Asn-224) localized between H2 and H3. Both our cloned

CSG1 gene and the gene registered in the *Saccharomyces* genome database (http://yeastgenome.org/) encode a Csg1 protein with 382 amino acid residues, whereas the amino acid sequence in that report contained only 381 residues (13). The missing amino acid residue is a Gly following the glycosylated Asn-224. Since *N*-glycosylation occurs on an Asn residue with the consensus sequence Asn-X-Thr or Asn-X-Ser, lack of the Gly residue must have resulted in the omission of Asn-224 as a potential *N*-glycosylation site. In the present study, we created an N224Q mutant and thereby determined that Asn-224 is indeed glycosylated (Fig. 6*B*). The second basis for the previous topology model was that in isolated membranes a C-terminal, 24 kDa band appeared following treatment with Trypsin. However, there are unsolved problems in the authors' interpretation. If their topology model was correct, the molecular mass of the protected band would be ~14 kDa. Moreover, the doublet bands corresponding to glycosylated and non-glycosylated bands unexpectedly became a single weak band upon treatment with Trypsin (13). Thus, it is unlikely that the 24 kDa band was a genuine, membrane-protected band.

The Ca^{2+}-sensitive phenotype of Δ*csg1* Δ*csh1* and Δ*csg2* cells is caused by an accumulation of IPC-C, which contains a ceramide composed of phytosphingosine and a monohydroxylated fatty acid (5-7). Previous reports have suggested that Ca^{2+} induces irreversible changes in the plasma membrane and/or cell wall in Δ*csg1* and Δ*csg2* cells that increases Ca^{2+} influx and leads to cell death (5). However, it is unclear whether Ca^{2+} directly perturbs the plasma membrane or affects its ion permeability through IPC-C-dependent signal transduction. The latter model, which we prefer, is supported by the fact that the Ca^{2+}-sensitive phenotype of the Δ*csg2* cells was suppressed by the mutations of two genes involved in signal transduction, the protein kinase *TOR2* and the phosphatidylinositol-4-phosphate 5-kinase *MSS4* (30). Phosphatidylinositol-4,5-bisphosphate (PtdIns(4,5)P_2) generated by Mss4 modulates several cellular events, including actin polarization and cell growth, via the Rho1 GTPase and Tor pathways (31-35). These signaling events are mediated by PtdIns(4,5)P_2-binding proteins (33-35). A recent study found that the plasma membrane localization of Mss4 is disturbed in Δ*csg2* cells (36), suggesting that accumulation of IPC-C or loss of MIPC causes mislocalization of Mss4. IPC-C contains three hydroxyl groups in the ceramide moiety and, thus, is predicted to interact, via hydrogen bonds, with other IPC-C molecules or with other lipid molecules that contain hydroxyl groups and/or amino groups, and thereby generate lipid microdomains. We speculate that Ca^{2+} binds to the phosphate group of IPCs and alters the lipid microdomain, leading to changes in the signaling pathways of Mss4 and Tor2.

Yeast microdomains are known to be composed of ergosterol and sphingolipids (2). We recently reported that a shift in the sphingoid base of the yeast sphingolipids from phytosphingosine/DHS to sphingosine disrupts the lipid microdomain (37). In that study we also demonstrated that yeast was highly sensitive to Ca^{2+}, suggesting a link between Ca^{2+}-sensitivity and lipid microdomain formation. However, further work will be required to confirm any involvement of lipid microdomains in the Ca^{2+}/IPC-C-mediated signal transduction pathway.

REFERENCES

1. Hakomori, S. (2004) *An. Acad. Bras. Cienc.* **76**, 553-572
2. Simons, K., and Toomre, D. (2000) *Nat. Rev. Mol. Cell Biol.* **1**, 31-39
3. Heidler, S. A., and Radding, J. A. (1995) *Antimicrob. Agents Chemother.* **39**, 2765-2769
4. Nagiec, M. M., Nagiec, E. E., Baltisberger, J. A., Wells, G. B., Lester, R. L., and Dickson, R. C. (1997) *J. Biol. Chem.* **272**, 9809-9817
5. Beeler, T. J., Fu, D., Rivera, J., Monaghan, E., Gable, K., and Dunn, T. M. (1997) *Mol. Gen. Genet.* **255**, 570-579
6. Haak, D., Gable, K., Beeler, T., and Dunn, T. (1997) *J. Biol. Chem.* **272**, 29704-29710
7. Dunn, T. M., Haak, D., Monaghan, E., and Beeler, T. J. (1998) *Yeast* **14**, 311-321
8. Stock, S. D., Hama, H., Radding, J. A., Young, D. A., and Takemoto, J. Y. (2000) *Antimicrob. Agents Chemother.* **44**, 1174-1180
9. Thevissen, K., Cammue, B. P., Lemaire, K., Winderickx, J., Dickson, R. C., Lester, R. L., Ferket, K. K., Van Even, F., Parret, A. H., and Broekaert, W. F. (2000) *Proc. Natl. Acad. Sci. U. S. A.* **97**, 9531-9536
10. Markovich, S., Yekutiel, A., Shalit, I., Shadkchan, Y., and Osherov, N. (2004) *Antimicrob. Agents Chemother.* **48**, 3871-3876
11. Zink, S., Mehlgarten, C., Kitamoto, H. K., Nagase, J., Jablonowski, D., Dickson, R. C., Stark, M. J., and Schaffrath, R. (2005) *Eukaryot. Cell* **4**, 879-889
12. Uemura, S., Kihara, A., Inokuchi, J., and Igarashi, Y. (2003) *J. Biol. Chem.* **278**, 45049-45055
13. Lisman, Q., Pomorski, T., Vogelzangs, C., Urli-Stam, D., de Cocq van Delwijnen, W., and Holthuis, J. C. (2004) *J. Biol. Chem.* **279**, 1020-1029
14. Beeler, T., Gable, K., Zhao, C., and Dunn, T. (1994) *J. Biol. Chem.* **269**, 7279-7284
15. Takita, Y., Ohya, Y., and Anraku, Y. (1995) *Mol. Gen. Genet.* **246**, 269-281
16. Abeliovich, H., Darsow, T., and Emr, S. D. (1999) *EMBO J.* **18**, 6005-6016
17. Levine, T. P., Wiggins, C. A., and Munro, S. (2000) *Mol. Biol. Cell* **11**, 2267-2281
18. Kihara, A., and Igarashi, Y. (2002) *J. Biol. Chem.* **277**, 30048-30054
19. Jungmann, J., and Munro, S. (1998) *EMBO J.* **17**, 423-434
20. Dean, N. (1999) *Biochim. Biophys. Acta.* **1426**, 309-322
21. Munro, S. (2001) *FEBS Lett.* **498**, 223-227
22. Meusser, B., Hirsch, C., Jarosch, E., and Sommer, T. (2005) *Nat. Cell Biol.* **7**, 766-772
23. Claros, M. G., and von Heijne, G. (1994) *Comput. Appl. Biosci.* **10**, 685-686
24. Reggiori, F., Canivenc-Gansel, E., and Conzelmann, A. (1997) *EMBO J.* **16**, 3506-3518
25. Reggiori, F., and Conzelmann, A. (1998) *J. Biol. Chem.* **273**, 30550-30559
26. Aerts, A. M., Francois, I. E., Bammens, L., Cammue, B. P., Smets, B., Winderickx, J., Accardo, S., De Vos, D. E., and Thevissen, K. (2006) *FEBS Lett.* **580**, 1903-1907
27. Ward, C. L., Omura, S., and Kopito, R. R. (1995) *Cell* **83**, 121-127
28. Hiller, M. M., Finger, A., Schweiger, M., and Wolf, D. H. (1996) *Science* **273**, 1725-1728
29. Yang, M., Omura, S., Bonifacino, J. S., and Weissman, A. M. (1998) *J. Exp. Med.* **187**, 835-846
30. Beeler, T., Bacikova, D., Gable, K., Hopkins, L., Johnson, C., Slife, H., and Dunn, T. (1998) *J. Biol. Chem.* **273**, 30688-30694
31. Desrivieres, S., Cooke, F. T., Parker, P. J., and Hall, M. N. (1998) *J. Biol. Chem.* **273**, 15787-15793
32. Homma, K., Terui, S., Minemura, M., Qadota, H., Anraku, Y., Kanaho, Y., and Ohya, Y. (1998) *J. Biol. Chem.* **273**, 15779-15786
33. Audhya, A., and Emr, S. D. (2002) *Dev. Cell* **2**, 593-605
34. Audhya, A., Loewith, R., Parsons, A. B., Gao, L., Tabuchi, M., Zhou, H., Boone, C., Hall, M. N., and Emr, S. D. (2004) *EMBO J.* **23**, 3747-3757
35. Fadri, M., Daquinag, A., Wang, S., Xue, T., and Kunz, J. (2005) *Mol. Biol. Cell* **16**, 1883-1900
36. Kobayashi, T., Takematsu, H., Yamaji, T., Hiramoto, S., and Kozutsumi, Y. (2005) *J. Biol. Chem.* **280**, 18087-18094

37. Tani, M., Kihara, A., and Igarashi, Y. (2006) *Biochem. J.* **394**, 237-242
38. Marck, C. (1988) *Nucleic Acids Res.* **16**, 1829-1836
39. Kyte, J., and Doolittle, R. F. (1982) *J. Mol. Biol.* **157**, 105-132
40. Irie, K., Takase, M., Lee, K. S., Levin, D. E., Araki, H., Matsumoto, K., and Oshima, Y. (1993) *Mol. Cell Biol.* **13**, 3076-3083
41. Brachmann, C. B., Davies, A., Cost, G. J., Caputo, E., Li, J., Hieter, P., and Boeke, J. D. (1998) *Yeast* **14**, 115-132
42. Winzeler, E. A., Shoemaker, D. D., Astromoff, A., Liang, H., Anderson, K., Andre, B., Bangham, R., Benito, R., Boeke, J. D., Bussey, H., Chu, A. M., Connelly, C., Davis, K., Dietrich, F., Dow, S. W., El Bakkoury, M., Foury, F., Friend, S. H., Gentalen, E., Giaever, G., Hegemann, J. H., Jones, T., Laub, M., Liao, H., Liebundguth, N., Lockhart, D. J., Lucau-Danila, A., Lussier, M., M'Rabet, N., Menard, P., Mittmann, M., Pai, C., Rebischung, C., Revuelta, J. L., Riles, L., Roberts, C. J., Ross-MacDonald, P., Scherens, B., Snyder, M., Sookhai-Mahadeo, S., Storms, R. K., Veronneau, S., Voet, M., Volckaert, G., Ward, T. R., Wysocki, R., Yen, G. S., Yu, K., Zimmermann, K., Philippsen, P., Johnston, M., and Davis, R. W. (1999) *Science* **285**, 901-906

FOOTNOTES

*This work was supported by a Grant-in-Aid for Young Scientists (A) (17687011) from the Ministry of Education, Culture, Sports, Sciences and Technology of Japan.

[1]To whom correspondence should be addressed. Tel.: 81-11-706-3971; Fax: 81-11-706-4986; E-mail: kihara@pharm.hokudai.ac.jp

[2]The abbreviations used are: GSLs, Glycosphingolipids; IPC, inositol phosphorylceramide; MIPC, mannosylinositol phosphorylceramide; $M(IP)_2C$, mannosyldiinositol phosphorylceramide; 3xFLAG, triple FLAG; HA, hemagglutinin; 3xHA, triple HA; PMSF, phenylmethylsulfonyl fluoride; PNGase F, peptide *N*-glycosidase F; DHS, dihydrosphingosine; ER, endoplasmic reticulum; ERAD, ER-associated degradation

ACKNOWLEDGMENT

We thank Dr. S. Munro for anti-Anp1 antibodies and Dr. A. Sweeney for editing the manuscript.

FIGURE LEGENDS

Fig. 1. *N*-glycosylation of Csg1 and Csh1. Control KA31-1A (*CSG1 CSH1*) cells and SUY69 (*CSG1-3xFLAG CSH1*) cells (*A*) or SUY73 (*CSG1 CSH1-3xFLAG*) cells (*B*) were grown at 30˚C in YPD medium. The fractions of integral membrane proteins were prepared and subjected to immunoprecipitation using anti-FLAG M2 antibodies. Immunoprecipitates, untreated or treated with PNGase F, were separated by SDS-PAGE and subjected to immunoblotting with anti-FLAG M2 antibodies. Csg1-3xFLAG* and Csh1-3xFLAG* indicate *N*-glycosylated forms of the proteins.

Fig. 2. Effect of Csg2 on the glycosylation status and protein levels of Csg1 and Csh1. *A,* SUY69

(*CSG1-3xFLAG CSG2*$^+$), SUY75 (*CSG1-3xFLAG* Δ*csg2*), SUY73 (*CSH1-3xFLAG CSG2*$^+$), and SUY80 (*CSH1-3xFLAG* Δ*csg2*) cells were grown at 30˚C in YPD medium. The fractions of integral membrane proteins were prepared and subjected to immunoprecipitation using anti-FLAG M2 antibodies. Immunoprecipitates were separated by SDS-PAGE, followed by immunoblotting with anti-FLAG antibodies. *B*, KA31-1A cells bearing pRS425 (vector) or pSU8 (*CSG2-3xHA*) were transfected with pSU30 (*CSG1-HIS$_6$-MYC*; upper panel) or pSU41 (*CSH1-HIS$_6$-MYC*; lower panel). Cells were grown at 30˚C in SC medium lacking histidine and leucine. The fractions of integral membrane proteins were prepared and subjected to immunoprecipitation using anti-Myc antibodies. Immunoprecipitates were separated by SDS-PAGE, and Csg1-His$_6$-Myc and Csh1-His$_6$-Myc were detected by immunoblotting with anti-Myc antibodies. Csg1-3xFLAG*, Csh1-3xFLAG*, Csg1-His$_6$-Myc*, and Csh1-His$_6$-Myc* indicate *N*-glycosylated forms of the proteins.

Fig. 3. Studies of *N*-glycan types in Csg1 and Csh1. *A*, Pathways and factors in the Golgi apparatus of *S. cerevisiae* involved in the maturation of two different *N*-linked glycans. The high mannose-type *N*-glycans are attached to the protein in the ER and are further modified in the Golgi. The *N*-glycans initially receive a single α-1,6-linked mannose by Och1. In 'mannan-type' structures, this mannose is extended to a long mannan backbone by the sequential action of two mannan polymerases (M-Pol)-I (a heterogenous dimeric enzyme containing Mnn9 and Van1) and M-Pol-II (a multi-complex enzyme containing Mnn9, Mnn10, Mnn11, Anp1, and Hoc1). The backbone is then branched with α-1,2-linked mannose by Mnn2 and Mnn5, and phosphomannose is added by Mnn6. Finally, the addition of α-1,6-linked mannose by Mnn1 terminates the 'mannan-type' synthesis. In contrast, the 'core-type' structure receives two mannoses by an unidentified enzyme and Mnn1. *B* and *C*, BY4741 (*VAN1*$^+$) and 7116 (Δ*van1*) cells, each bearing pSU8 (*CSG2-3xHA*), were transfected with pSU30 (*CSG1-HIS$_6$-MYC*) (*B*) or pSU41 (*CSH1-HIS$_6$-MYC*) (*C*). Cells were grown at 30˚C in SC medium lacking histidine and leucine. The fractions of integral membrane proteins were prepared, and Csg1-His$_6$-Myc and Csh1-His$_6$-Myc were immunoprecipitated with anti-Myc antibodies. Immunoprecipitates were separated by SDS-PAGE, and proteins were detected by immunoblotting with anti-Myc antibodies. Csg1-His$_6$-Myc* and Csh1-His$_6$-Myc* indicate *N*-glycosylated forms of the proteins.

Fig. 4. An essential role for Csg2 in the exit of Csh1 from the ER. SUY73 (*CSH1-3xFLAG CSG2*$^+$) and SUY80 (*CSH1-3xFLAG* Δ*csg2*) cells were grown at 30˚C in YPD medium. Cell lysates were fractionated on a sucrose density gradient. Fractions were analyzed by immunoblotting with anti-FLAG, anti-Anp1, and anti-Dpm1 antibodies. Anp1 and Dpm1 were utilized as specific markers for the Golgi and ER, respectively. Csh1-3xFLAG (M) and Csh1-3xFLAG (H) indicate proteins carrying N-glycans of mannan-type and high mannose-type, respectively.

Fig. 5. Differing effects of Csg2 on the degradation of Csg1 and Csh1 in the vacuole. *A and B,* Csg1-3xFLAG-expressing cell lines SUY69 (*CSG2*$^+$ *PEP4*$^+$ *PRB1*$^+$), SUY96 (*CSG2*$^+$ Δ*pep4* Δ*prb1*), and SUY99 (Δ*csg2* Δ*pep4* Δ*prb1*) (*A*) and Csh1-3xFLAG-expressing cell lines SUY73 (*CSG2*$^+$ *PEP4*$^+$ *PRB1*$^+$), SUY98 (*CSG2*$^+$ Δ*pep4* Δ*prb1*), and SUY100 (Δ*csg2* Δ*pep4* Δ*prb1*) (*B*) were grown at 30˚C in YPD medium. The fractions of integral membrane proteins were subjected to immunoprecipitation

with anti-FLAG M2 antibodies. Immunoprecipitates were separated by SDS-PAGE, and Csg1-3xFLAG and Csh1-3xFLAG were detected by immunoblotting with anti-FLAG M2 antibodies. Csg1-3xFLAG* and Csh1-3xFLAG* indicate *N*-glycosylated forms of the proteins; Csg1-3xFLAG** and Csh1-3xFLAG** denote possible degradation products; (•) indicates non-specific bands.

Fig. 6. *N*-glycosylation sites and predicted transmembrane topology of Csh1 and Csg1. *A*, Hydrophobic profiles of Csh1 (upper panel) and Csg1 (lower panel) were obtained using the DNA Strider program version 1.2 (38) with Kyte and Doolittle hydrophilicity values (39). H*n* represents a potential transmembrane-spanning domain as predicted by the TopPredII 1.1 program (23). M denotes the conserved mannosyltransferase domain. The position of each asparagine residue that is a potential *N*-glycosylation site is also indicated with its amino acid number. *B*, KA31-1A cells bearing pSU8 (*CSG2-3xHA*) were transfected with pSU41 (*CSH1-HIS$_6$-MYC*), pSU108 (*CSH1-N51Q-HIS$_6$-MYC*), pSU109 (*CSH1-N247Q-HIS$_6$-MYC*), pSU193 (*CSH1-N51/247Q-HIS$_6$-MYC*), pSU30 (*CSG1-HIS$_6$-MYC*), or pSU145 (*CSG1-N224Q-HIS$_6$-MYC*). The fractions of integral membrane proteins prepared from these cells were subjected to immunoprecipitation with anti-Myc antibodies. Immunoprecipitates were separated by SDS-PAGE, and proteins were detected by immunoblotting with anti-Myc antibodies. *C*, A model for the transmembrane topology of Csh1 and Csg1. Csh1 and Csg1 are integral membrane proteins with two (H1 and H3) or one (H3) transmembrane domain. The C-termini are located in the cytosol, and the mannosyltransferase domains (M) are located in the lumen.

Fig. 7. Ca^{2+}-dependent increases in Csg1 protein levels. *A*, Csg1-3xFLAG-expressing cell lines SUY69 (*CSG2*$^+$) and SUY75 (Δ*csg2*), Csh1-3xFLAG-expressing cell lines SUY73 (*CSG2*$^+$) and SUY80 (Δ*csg2*), and the Csg2-3xFLAG-expressing cell line SUY71 (*CSG2*$^+$) were grown at 30˚C for 3 h in YPD medium containing 0, 0.1, 1, 10, or 100 mM $CaCl_2$. The fractions of integral membrane proteins were prepared, treated with PNGase F to remove *N*-glycans, and separated by SDS-PAGE. Proteins were detected by immunoblotting with anti-FLAG antibodies or, to demonstrate uniform protein loading, anti-Dpm1 antibodies. *B*, KA31-1A cells were grown for 3 h at 30˚C in YPD medium containing 0, 0.1, 1, 10, or 100 mM $CaCl_2$. Total RNA was prepared from these cells, converted to cDNA, and subjected to real-time PCR using primers and probes specific for *CSG1*, *CSH1*, *CSG2*, or *ACT1* (*actin*). Values presented are *CSG1*, *CSH1*, and *CSG2* mRNA levels relative to the level of *ACT1* mRNA. All values represent a mean ± SD from three independent experiments.

Fig. 8. Stimulation of MIPC synthesis by Ca^{2+} treatment. KA31-1A cells grown in YPD medium were incubated with 0, 10, or 100 mM $CaCl_2$ for 1 h at 30˚C. Cells were then labeled with [^{3}H]DHS for 3 h at 30˚C. Lipids were extracted and separated by TLC with chloroform/methanol/4.2 N ammonia (9/7/2, v/v/v) (upper panel). Since IPC-D and MIPC-A, as well as B and B' species, are not separated by this solvent system, lipids were also resolved by chloroform/methanol/acetic acid/water (16/6/4/1.6, v/v/v/v) (lower panel). Labeled lipids were detected by autoradiography. The asterisk indicates unidentified metabolites of DHS.

TABLE I. *Yeast strains used in this study*

Strain	Genotype	Source
KA31-1A	*MAT**a** ura3 leu3 his3 trp1*	Ref. 40
BY4741	*MAT**a** his3Δ1 leu2Δ0 met15Δ0 ura3Δ0*	Ref. 41
7116	BY4741, Δ*van1*::*KanMX4*	Ref. 42
SUY69	KA31-1A, *csg1*::*CSG1-3xFLAG HIS3*	This study
SUY71	KA31-1A, *csg2*::*CSG2-3xFLAG HIS3*	This study
SUY73	KA31-1A, *csh1*::*CSH1-3xFLAG HIS3*	This study
SUY75	KA31-1A, *csg1*::*CSG1-3xFLAG HIS3* Δ*csg2*::*URA3*	This study
SUY80	KA31-1A, *csh1*::*CSH1-3xFLAG HIS3* Δ*csg2*::*URA3*	This study
SUY96	KA31-1A, *csg1*::*CSG1-3xFLAG HIS3* Δ*pep4*::*LEU2* Δ*prb1*::*KanMX4*	This study
SUY98	KA31-1A, *csh1*::*CSH1-3xFLAG HIS3* Δ*pep4*::*LEU2* Δ*prb1*::*KanMX4*	This study
SUY99	KA31-1A, *csg1*::*CSG1-3xFLAG HIS3* Δ*csg2*::*URA3* Δ*pep4*::*LEU2* Δ*prb1*::*KanMX4*	This study
SUY100	KA31-1A, *csh1*::*CSH1-3xFLAG HIS3* Δ*csg2*::*URA3* Δ*pep4*::*LEU2* Δ*prb1*::*KanMX4*	This study

Figure 1

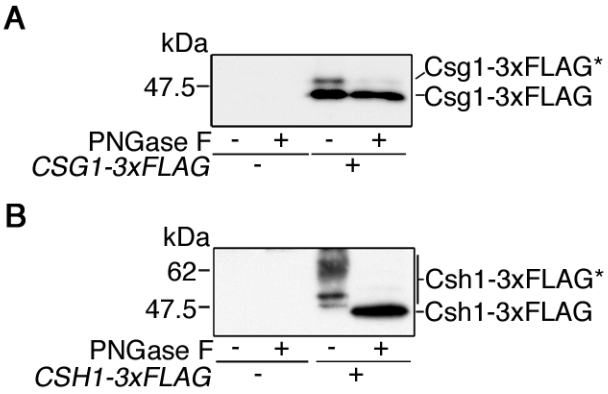
A
kDa
47.5
Csg1-3xFLAG*
Csg1-3xFLAG
PNGase F - + - +
CSG1-3xFLAG - +
B
kDa
62
47.5
Csh1-3xFLAG*
Csh1-3xFLAG
PNGase F - + - +
CSH1-3xFLAG - +

Figure 2

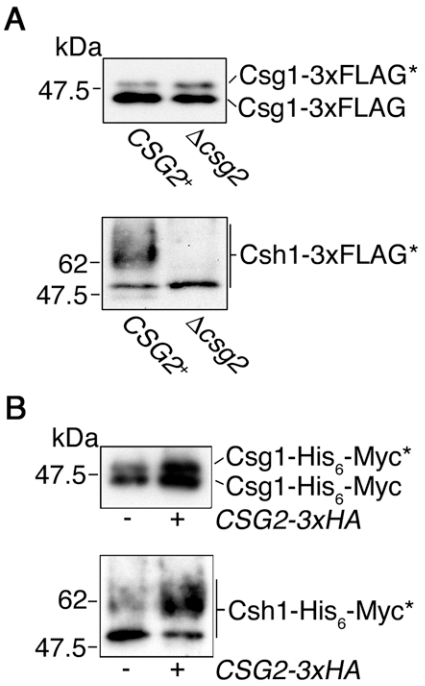
A
kDa
47.5
Csg1-3xFLAG*
Csg1-3xFLAG
CSG2+
Δcsg2
62
47.5
Csh1-3xFLAG*
CSG2+
Δcsg2
B
kDa
47.5
Csg1-His6-Myc*
Csg1-His6-Myc
- +
CSG2-3xHA
62
47.5
Csh1-His6-Myc*
- +
CSG2-3xHA

Figure 3

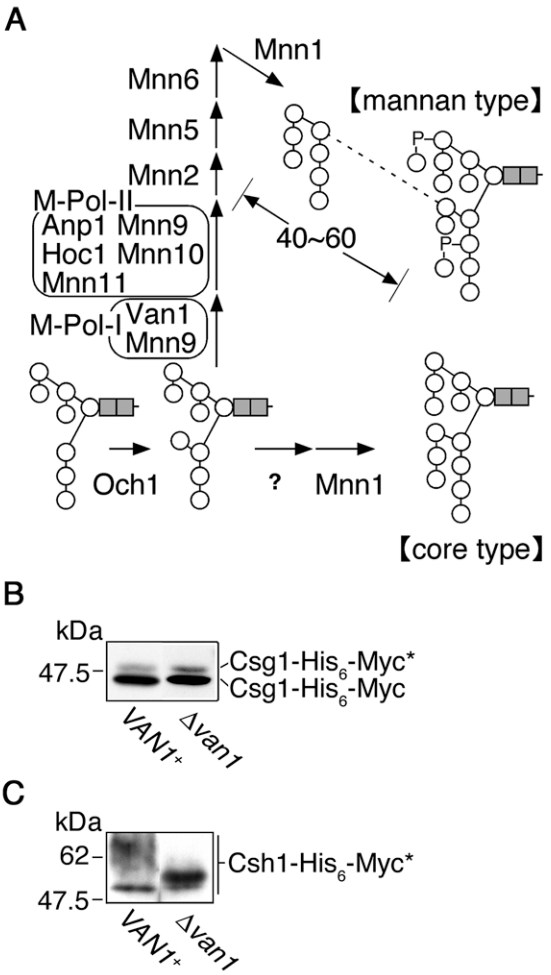
A
Mnn1
Mnn6
【mannan type】
Mnn5
Mnn2
M-Pol-II
Anp1 Mnn9
Hoc1 Mnn10
Mnn11
40~60
M-Pol-I
Van1
Mnn9
Och1
?
Mnn1
【core type】
B
kDa
47.5
Csg1-His6-Myc*
Csg1-His6-Myc
VAN1+
Δvan1
C
kDa
62
47.5
Csh1-His6-Myc*
VAN1+
Δvan1

Figure 4

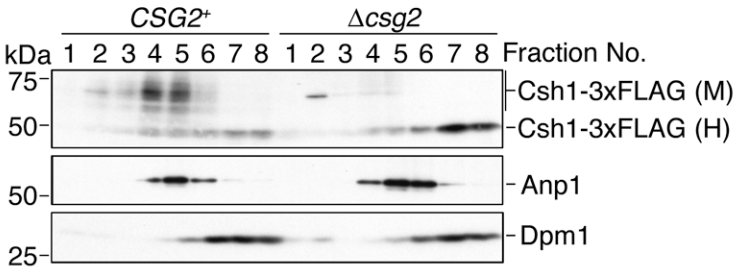
CSG2+
Δcsg2
kDa
1 2 3 4 5 6 7 8 1 2 3 4 5 6 7 8
Fraction No.
75
50
50
25
Csh1-3xFLAG (M)
Csh1-3xFLAG (H)
Anp1
Dpm1

Figure 5

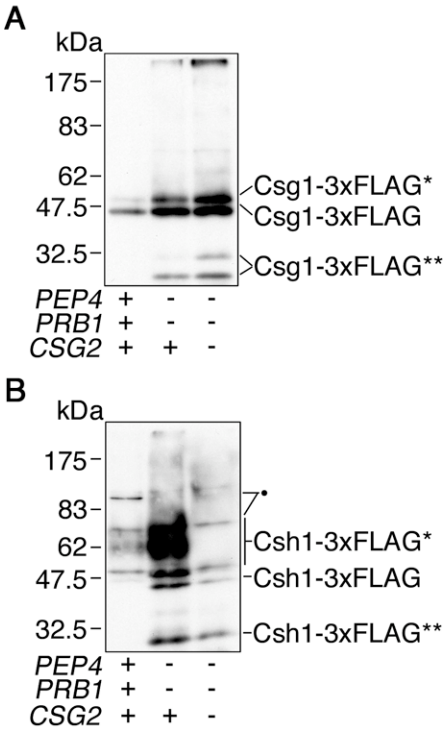
A
kDa
175
83
62
47.5
32.5
Csg1-3xFLAG*
Csg1-3xFLAG
Csg1-3xFLAG**
PEP4 + - -
PRB1 + - -
CSG2 + + -
B
kDa
175
83
62
47.5
32.5
Csh1-3xFLAG*
Csh1-3xFLAG
Csh1-3xFLAG**
PEP4 + - -
PRB1 + - -
CSG2 + + -

Figure 6

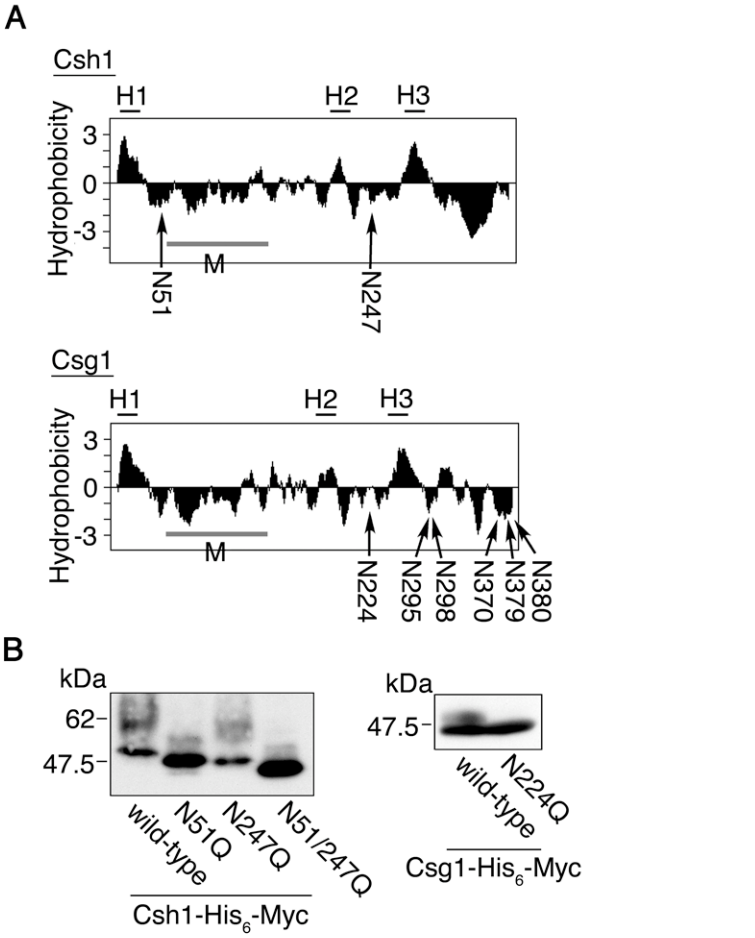
A
Csh1
H1
H2
H3
Hydrophobicity
3
0
-3
M
N51
N247
Csg1
H1
H2
H3
Hydrophobicity
3
0
-3
M
N224
N295
N298
N370
N379
N380
B
kDa
62
47.5
wild-type
N51Q
N247Q
N51/247Q
Csh1-His6-Myc
kDa
47.5
wild-type
N224Q
Csg1-His6-Myc
C
Csh1
N
C
H1
H2
H3
M
or
cytosol
Gogi membrane
lumen
Csg1
N
C
H1
H2
H3
M
or
cytosol
Gogi membrane
lumen

Figure 7

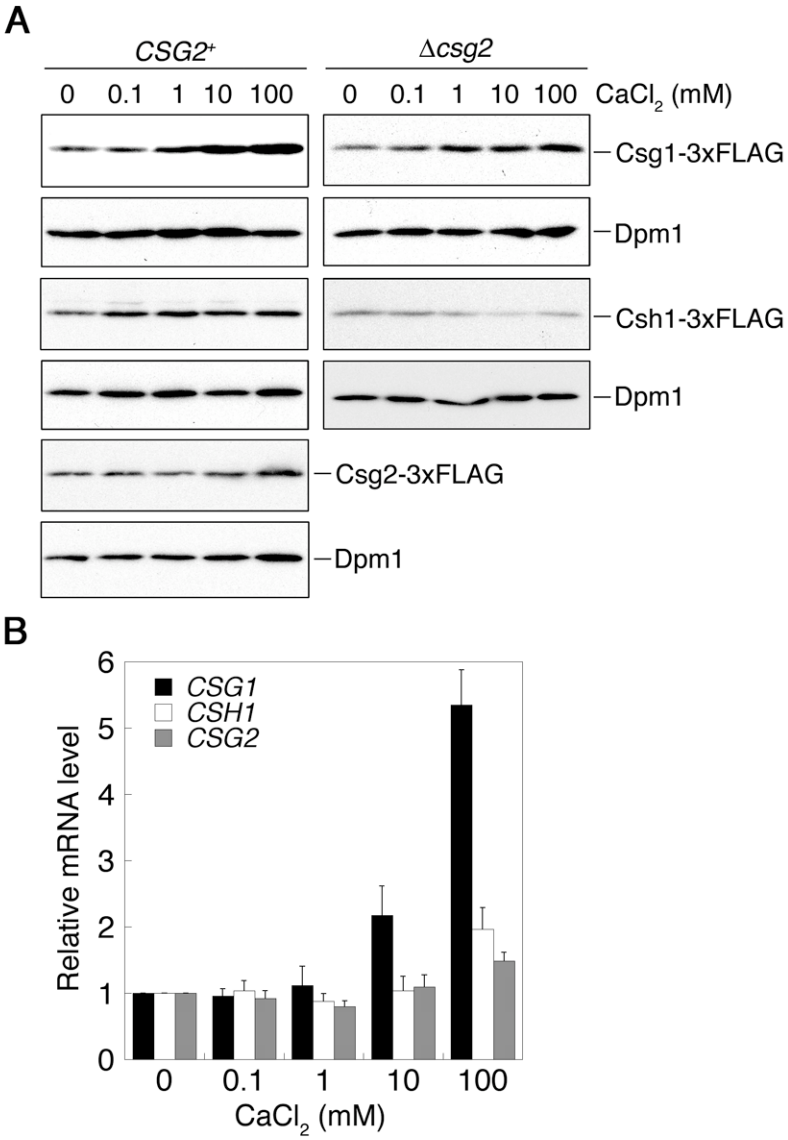
A
CSG2+
Δcsg2
0 0.1 1 10 100
0 0.1 1 10 100
CaCl2 (mM)
Csg1-3xFLAG
Dpm1
Csh1-3xFLAG
Dpm1
Csg2-3xFLAG
Dpm1
B
CSG1
CSH1
CSG2
Relative mRNA level
0 1 2 3 4 5 6
0 0.1 1 10 100
CaCl2 (mM)

Figure 8

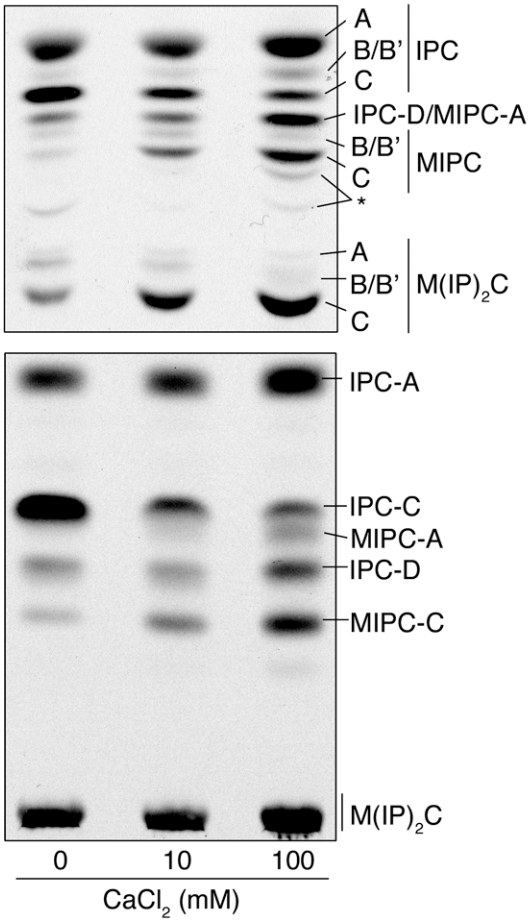
A
B/B'
C
IPC
IPC-D/MIPC-A
B/B'
C
*
MIPC
A
B/B'
C
M(IP)2C
IPC-A
IPC-C
MIPC-A
IPC-D
MIPC-C
M(IP)2C
0
10
100
CaCl2 (mM)